Schnepp, E., Leonhardt, R., Korte, M., Klett-Drechsel, J. (2016): Validity of archaeomagnetic field recording: an experimental pottery kiln at Coppengrave, Germany. - *Geophysical Journal International*, *205*, 1, pp. 622–635.

DOI: http://doi.org/10.1093/gji/ggw043

Geophysical Journal International

Geophys. J. Int. (2016) **205,** 622–635
Advance Access publication 2016 January 27
GJI Geomagnetism, rock magnetism and palaeomagnetism

doi: 10.1093/gji/ggw043

Validity of archaeomagnetic field recording: an experimental pottery kiln at Coppengrave, Germany

Elisabeth Schnepp,[1] Roman Leonhardt,[2] Monika Korte[3] and Johannes Klett-Drechsel[4]

[1]*Palaeomagnetic Laboratory Gams, Chair of Geophysics, University of Leoben, Gams* 45, *A*-8170 *Frohnleiten, Austria, E-mail: elisabeth.schnepp@unileoben.ac.at*
[2]*Zentralanstalt für Meteorologie und Geodynamik, CONRAD Observatorium, Hohe Warte* 38, 1190 *Wien, Austria*
[3]*Deutsches GeoForschungsZentrum GFZ, Behlertstraße* 3*a, D*-14467 *Potsdam, Germany*
[4]*KERAMIK UM, Ausstellungs- und Aktionshaus Fredelsloh, Am Kapellenbrunnen* 5, *D*-37186 *Fredelsloh, Germany*

Accepted 2016 January 25. Received 2016 January 25; in original form 2015 July 14

SUMMARY

Palaeomagnetic data obtained from archaeological materials are used for reconstructions of the Earth's magnetic field of the past millennia. While many studies tested the reliability of this recorder for palaeointensity only a few studies did this for direction. The study presents an archaeomagnetic and rock magnetic investigation applied to an experimental pottery kiln, which was operated in 2003 to produce stone ware. This kind of high-quality pottery needs a temperature of at least 1160 °C. Shortly before heating of the kiln direct absolute measurements of the absolute geomagnetic field vector have been carried out close to it. After cooling of the kiln 24 oriented palaeomagnetic samples have been taken. Although Curie temperatures are about 580 °C, that is the typical temperature for magnetite, thermal as well as alternating field demagnetisations reveal also a considerable amount of hematite as magnetic carrier. This mixture of magnetite and hematite is dominated by pseudo-single domain grains. Demagnetisation removed in some cases weak secondary components, but in most cases the specimens carried a single component thermoremanent magnetisation. The mean characteristic remanent magnetisation direction agrees on 95 per cent confidence level with the directly measured field direction. Archaeointensity was obtained from five specimens with the Thellier–Coe method and with the multiple-specimen palaeointensity domain-state corrected method. Six of these specimens also provided a result of the Dekkers–Böhnel method, which overestimated the archaeointensity by about 9 per cent compared to the direct value, while after correction for fraction the value agrees very well. For the multiple-specimen palaeointensity domain-state corrected method only fractions between 25 and 75 per cent have been used and specimens showing alteration have been excluded. Above 450 °C many specimens showed alteration of the magnetic grains. Because median destructive temperatures were often above this value in most cases the fraction was less than 50 per cent. Nevertheless the obtained intensity (48.48 ± 0.24 μ) is on 95 per cent confidence level in agreement with the direct observation. Behaviour of the specimens during the Thellier-experiments was not ideal because of narrow unblocking temperature spectra and alteration. Nevertheless, the obtained mean archaeointensity is also in agreement with the direct field observation. Here the relative palaeointensity error is about 6 per cent and very high compared the multiple-specimen palaeointensity domain-state corrected method. The investigation demonstrates that a pottery kiln can provide a very precise estimate of the ancient geomagnetic field vector.

Key words: Archaeomagnetism; Palaeointensity; Palaeomagnetic secular variation.

INTRODUCTION

The fundamental hypothesis of palaeo- and archaeomagnetism is that (1) a geological or archaeological structure like a lava flow or a kiln will gain a magnetization parallel to the ambient local magnetic field of the Earth when it cools down and (2) the palaeomagnetic investigation of oriented samples provides direction and intensity of the geomagnetic field at the time when the last cooling took place. While many tests of such a quality control exist for lavas (i.e. Tanguy *et al.* 2003; Herrero-Bervera & Valet 2009; Ferk

et al. 2012; Cromwell *et al.* 2015) and archaeointensity (Genevey & Gallet 2002; Aidona *et al.* 2008; Catanzariti *et al.* 2008; Morales *et al.* 2011; Yamamoto *et al.* 2015) such investigations on direction of archaeological structures have seldom been carried out. Soffel & Schurr (1990) studied two models of kilns with a scale of 1:10 made of clay enriched with iron oxide in order to investigate magnetic refraction. Although they observed large deviations, the mean directions were close to the magnetising field. For two experimental kilns the authors (Nakajima *et al.* 1974; Catanzariti *et al.* 2008) concluded that the geomagnetic direction was recorded correctly.

Experimental archaeology tries to understand how our ancestors had manufactured the finds which were discovered in archaeological excavations. This is done by reproducing the techniques according to the knowledge which is provided by the features that were excavated or by historical documents. For the production of medieval pottery many examples of kilns can be consulted. The kiln used in this study was designed in order to reproduce stoneware, which is a vitreous, tight ceramic, known as the qualitatively best available during medieval times. For production of this kind of pottery the firing temperature must be as high as 1160 °C. The occurrence of stoneware in archaeological sites of the Rhineland starts in the 13th century AD, in Lower Saxony the sites are somewhat younger and this type of pottery is accompanied by an advanced technique and construction of the kilns. The kiln used in this study was built to celebrate the 600 yr jubilee of the village Coppengrave in 2000. The project tied up to about 800 yr of pottery tradition in this region. The kiln was regularly used once a year between 2000 and 2005.

After the experimental kiln's operation in summer 2003, it was sampled for an 'archaeomagnetic' investigation, in order to compare mean values of direction and intensity obtained palaeomagnetically with direct absolute measurements of the ambient magnetic field, which were carried out about one week before firing of the kiln. Palaeointensity was determined using the multiple-specimen absolute palaeointensity method proposed by Fabian & Leonhardt (2010) and Thellier experiments as well. Characteristic remanent magnetization direction was obtained by application of standard procedures. A rock magnetic characterization is provided as well.

THE EXPERIMENTAL POTTERY KILN AT COPPENGRAVE

The structure and technique of the experimental pottery kiln at Coppengrave is based on investigations of medieval pottery kilns in the south of Lower Saxony which had been excavated at Coppengrave, Fredelsloh/Bengerode and the region of the Reinhardswald on the territory of the Earl of Dassel (Stephan 2010). None of these examples had been in a good state of preservation and provided only vague information about what the kilns originally looked like. Hence, the reconstruction of the kiln's cupola, smokestack, access to the firing cavity and control of firing was completed with essential information from historical tradition and kilns using wood firing, which exist in eastern Asia.

A detailed description of the experimental kiln at Coppengrave was given by Brosch *et al.* (2003), which is summarized here. The kiln is composed of a working pit, the combustion space, the firing cavity and a flue (Figs 1a and b). The kiln's firing cavity has a volume of about 1 m^3 and the floor has a slope of about 20°. For the construction of the firing cavity 300 osier stakes, thick as a thumb and bent in arcs, formed the skeletal structure of the kiln's cupola. A mortar composed of 5500 kg clay, 1000 kg husk and 1 m^3 of sand and water was applied to form the walls, cupola and smokestack. The combustion space and the firing cavity are separated by five columns made of pots, which were plastered with kiln-loam. The direct access to the firing cavity had no antetype found in archaeological excavations, at that time, and was built for practical reasons. Meanwhile, such a door was found in a kiln excavated at Fredelsloh in 2005. It was closed with loam bricks after placing about 360 pots in the firing cavity (Figs 1c and d). Operation of the kiln takes about 6.5 m^3 of solid beech timber (Fig. 1e). After about 13 hr of firing the entire firing cavity is filled with flue gas and so-called 'firefoxes' appear in the vents, which allow regulation of oxygen entrance (Fig. 1f) and to observe the pyrometric cones used for checking the sintering process of the ceramics. The kiln temperature was measured with three thermocouples distributed along the firing cavity. After about 20 hr of firing a maximal temperature of 1153 °C was reached (Fig. 2) in the middle of the kiln where one thermocouple was placed. That third of the firing cavity, which is close to the combustion chamber reaches a somewhat higher temperature which is needed to produce stoneware. Then also the entrance of the combustion space was closed with loam bricks. After that the kiln cooled down for nearly 3 d, then the access to the firing cavity was opened and the pottery (Fig. 1g) could be removed. Because the columns of pots are often not stable, some toppled down. This may explain the large amounts of waster, which were found at the archaeological excavations of such kilns. In 2003, the production yielded about one third vessels of stoneware and the rest were vessels of earthenware, which are produced in the cooler parts of the firing cavity. They are of lower quality because earthenware is not water-tight.

DIRECT ABSOLUTE MEASUREMENTS OF THE MAGNETIC FIELD

Current geomagnetic main field models like the International Geomagnetic Reference Field (IGRF, Finlay *et al.* 2010) provide strength and directions of the core field, but do not take into account potential local crustal anomalies or influences from external magnetic field contributions. Direct observations of the geomagnetic field were carried out near the kiln shortly before the archaeomagnetic experiment in order to confirm the IGRF values and obtain an improved accuracy of magnetic field information during the time when our samples acquired their magnetization.

Direct observations were carried out following standard techniques for absolute field measurements at magnetic observatories or repeat stations (Newitt *et al.* 1996), using a Zeiss theodolite with Bartington fluxgate sensor for directional and a GEM Systems GSM 19 Overhauser magnetometer for intensity determinations. In order to check that the location is free of strong local crustal field anomalies a rough survey was carried out with the GSM 19 magnetometer over an area of several meters squared. Intensity gradients proved to be low, in the order of few nT per meter at most. Field intensity was monitored continuously during the directional measurements on a tripod 10 m away and corrected by the site difference which had been determined as 25 nT before and after the directional observations. An azimuth mark as geographic reference for the declination observations was determined by means of a north-seeking gyro-theololite (Sokkia theodolite set 31000), which from experience provides an accuracy better than 20 arcsec. One set of declination and inclination observations was performed with the Zeiss theodolite by an experienced observer. The absolute measurements were carried out on 2003 August 24 between 11:44

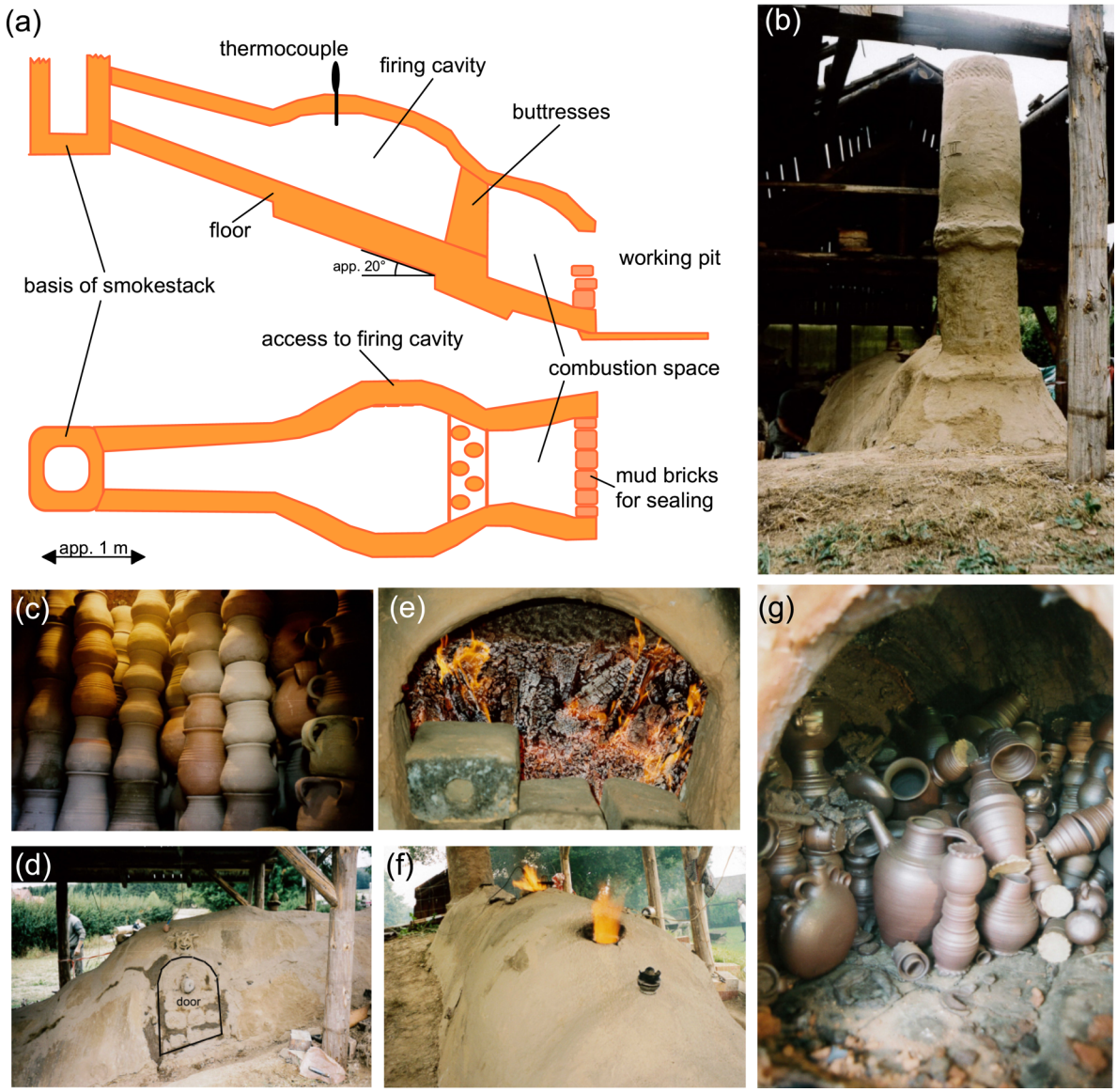

Figure 1. The experimental kiln at Coppengrave: (a) sketch (redrawn from Brosch *et al.* 2003), (b) view with flue, (c) pots stocked before firing, (d) closed door, (e) combustion chamber, (f) firefoxes during operation, (g) pottery, which was produced.

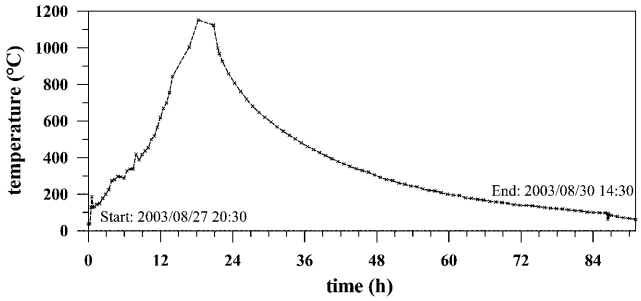

Figure 2. Temperature during heating and cooling of the kiln is plotted versus time. Position of the thermocouple is shown in Fig. 1(a).

and 12:16 UT. Data processing follows the standard geomagnetic observatory method (e.g. Jankowski & Sucksdorff 1996). The declination, inclination and intensity results reported in Table 1 are reduced to 11:57 UT on 2003 August 24 using variation recordings of the Adolf-Schmidt-Observatory for Geomagnetism in Niemegk of Helmholtz-Center Potsdam, German Research Center for Geosciences at about 200 km distance. Magnetic conditions were quiet during this and the following days, the variations from August 24th to August 30th did not exceed 27 arcmin in declination, 8 arcmin in inclination and 60 nT in intensity. This is below the resolution that can be obtained from archaeomagnetic experiments. We therefore do not need to reduce the results from the direct measurements further or consider uncertainties of the direct observations, which lie well below the daily variations.

SAMPLING AND ARCHAEOMAGNETIC INVESTIGATION

Ten large block samples have been taken with a modified Thellier technique (Schnepp *et al.* 2008) and a plane plaster surface for orientation was prepared while 14 small samples were obtained

Table 1. Magnetic field direction at Coppengrave (51.989°N, 9.721°E): Kind of measurement; calendar date; number of samples; number of independent characteristic remanent magnetization (ChRM) directions; declination; inclination; precision parameter; α_{95} confidence limit, intensity.

Measure	Date	n	N	D (°)	I (°)	k	α_{95} (°)	F (μT)
Archaeomagnetic	2003/08/28-30	24	20	1.9	66.1	481	1.5	48.5 ± 0.2
Direct	2003/08/24	–	–	0.725	67.232	–	–	48.735
IGRF	2003/08/23-30	–	–	0.768	67.217	–	–	48.830

with a somewhat different technique. To do so, glass discs of 25 mm diameter were glued with plaster on the inner surface of the kiln. For this purpose only cracked parts could be taken which allowed for removing the sample without further demolishing of the kiln. Samples have been taken from the floor (6), from the walls (10) and from the ceiling (8), and oriented with a magnetic compass and inclinometer. For two samples close to the door the azimuth was also measured with a sun compass. No important deviation compared to the magnetic compass was observed ($\leq 1°$).

Because the material was very hard and more like brick than baked clay no consolidation was necessary and cutting was done with a water cooled diamond saw. For the 'Thellier technique' blocks no further preparation was needed, while the other relatively small samples were first embedded into larger plaster blocks. After that all the blocks were cut into cubes of 20 mm edge length. Three pure plaster specimens were also prepared in order to check their magnetization intensity. For most of the specimens it turned out to be two to three orders of magnitude lower than the NRM of the kiln material. No specimens had to be excluded because of their low intensity and large amount of plaster.

The archaeomagnetic investigation started with measurements of mass, natural remanent magnetization (NRM), and bulk susceptibility using a 2G-Cryogenic magnetometer and an Agico minikappa bridge. Alternating field (AF) demagnetization was done with a 2 G demagnetizer in line with the magnetometer. For thermal demagnetization and the palaeointensity experiments a Magnetic Measurements MMTD80 furnace was used. In order to characterize the rock magnetic carriers, thermomagnetic curves of susceptibility were measured with an Agico MFK1, frequency and field dependence of susceptibility was recorded using a Magnon Susceptibility Bridge (VFSM), and hysteresis parameters were determined using a LOT-Quantum Design vibrating sample magnetometer (VSM).

Apart from a standard palaeo- and rock magnetic investigation in order to obtain the archaeomagnetic direction and information on its magnetic carrier, palaeointensity experiments have been carried out on five specimens using the Coe (1967) variation of the Thellier method. 13 temperature steps between 100 and 600 °C were measured, starting with a step in zero-field followed by heating and cooling in a field of 30 μT. Moreover, the protocol included 6 pTRM-checks, 5 tail-checks (Riisager & Riisager 2001) and 4 additivity-checks (Krása *et al.* 2003).

Furthermore, the multiple-specimen palaeointensity domain-state corrected method (MSP-DSC, Fabian & Leonhardt 2010) was applied on 2–19 specimens obtained from five different blocks. For this purpose it is necessary to adjust the laboratory field H_{Lab} (anti-)parallel with the anisotropy-corrected NRM direction of each specimen. Their anisotropy was investigated by imparting anhysteretic remanent magnetizations (ARM) using a Magnon International AFD 300 demagnetizer with 150 mT AF field and 50 μT constant magnetic field in six directions (+X, −X, +Y, −Y, +Z, −Z). Possible alteration of the AF coecivity spectrum of ARM was checked after heating the specimens to 250, 350 and 450 °C with AF demagnetization steps of 10, 35, 100, and 250 mT, respectively.

The ARM tensor and the corrected NRM directions (NRM_{ac}) of sister specimens used for the MSP-DSC experiments were calculated following Veitch *et al.* (1984). During the MSP-DSC experiments adjustment of the NRM_{ac} direction (anti-)parallel to the H_{Lab} was achieved by a special device built for cubic specimens with 13 mm edge length by the institute workshop. It is similar to that used by Böhnel *et al.* (2009) and fits with 8 specimens into a MMTD80 furnace. The following five steps have been performed for each specimen: (1) measurement of NRM; (2) measurement of the pTRM imparted parallel to the NRM_{ac} at a temperature T with heating and cooling in $+H_{Lab}$; (3) measurement of the pTRM imparted antiparallel to the NRM_{ac} at the same temperature T with heating and cooling in the field $-H_{Lab}$; (4) measurement of the pTRM imparted parallel to the NRM_{ac} at the same temperature T with heating in zero field and cooling in the same $+H_{Lab}$; (5) same as (2). These steps were performed at various temperatures between 300 and 510 °C and H_{Lab} was chosen between 15.5 and 102.3 μT. The first two steps are similar to a multiple-specimen palaeointensity experiment as proposed by Dekkers & Böhnel (2006), but in the present study the temperature is not adjusted close to MDT, it can be lower in order to avoid alteration or higher as well. Nevertheless, in the following this step will be called DB-step. The first three steps are the same as for a Thellier experiment. Therefore the third step will be called TH-step. This step provides control on the fraction which was remagnetized during the experiment, and provides the directions of the imparted pTRM as well as of the NRM left after its emplacement. The forth step is a zero-field heating step (ZF-step) and it tests in combination with the DB-step if the unblocking processes are the same during in-field heating as during zero-field heating. According to fig. 3 of Fabian & Leonhardt (2010) the remanence gained here must be smaller than for in-field heating. If this is not the case alteration enhancing the TRM-capacity of the specimen already took place. Hence the ZF-step is a combination of testing the presence of MD grains or alteration. The last step (RP-step) reproduces the DB-step in order to test reproducibility of the pTRM and indicates therefore any alteration and thermal stabilization. All these tests allow defining hard criteria, which are automatically applied to the measurements to weight data points and they are used to correct for fraction and MD-effects.

RESULTS AND DISCUSSION

Direction

NRM directions plotted in Fig. 3 cluster close to the present day magnetic field direction but also some displaced data points are present. According to generally high (9.7–65.9, *cf.* Schnepp *et al.* 2004) Koenigsberger ratios (Fig. 4a) insufficient heating is an unlikely explanation for these distorted directions.

AF (24 specimens) and thermal (seven specimens) demagnetizations revealed very stable directions with only minor secondary components. Fig. 5 shows eight examples, which show that both

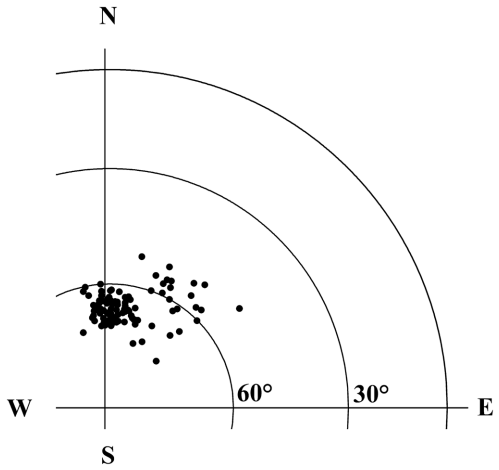

Figure 3. Natural remanent magnetization (NRM) directions are shown in equal area projection.

demagnetization methods yield the same direction for specimens from different samples (a and c) as well as within a sample (d). Small secondary components are present in many of the specimens (a, c and d) but only in a few cases (b) the direction changed considerably. These secondary components can be explained by a viscous magnetization acquired during stocking of the samples in the laboratory in arbitrary directions. Only for specimen CG-16-C12 the secondary component may be explained by the weak magnetization of the kiln fragment and the large amount of plaster, which carried a soft magnetization. Specimen CG-12-B11 (c) is one of those specimens with distorted NRM but here the direction remains unchanged after demagnetization. With the exception of one specimen a relatively hard magnetic component is present in all others, that is seen from residual magnetizations of between 15 and 65 per cent of the NRM left at 120 mT AF peak field. Nevertheless most specimens are demagnetized at 600 °C and only in a few cases 700 °C are needed. The characteristic remanent magnetization (ChRM) directions have been obtained from principal component analysis (PCA, Kirschvink 1980) using 6–12 demagnetization steps. In one case only three steps were used because the specimen was broken during the experiment. Maximum angular deviation was between 0.1° and 1.9° and in most cases less than 0.5° underlining the stability of the magnetizations.

After demagnetization the distribution of directions remains more or less unchanged (Fig. 6). There is still a cluster and 8 directions relatively far away from it. One of these aberrant directions has been obtained from a sample for which measuring the dip in the field was very difficult, in two cases the sampled material was relatively loose, while three come from material that was slightly displaced during embedding it into plaster in the laboratory. These six distorted directions have been tested using the outlier test of McFadden (1982) and all have been rejected on the basis of the test. The mean direction was calculated by averaging specimens from the same samples first and then all the independently oriented sample directions. The mean direction is given in Table 1 and shown in Fig. 6. Table 1 lists also the result obtained from the direct absolute measurement as well as the direction retrieved from the online field calculator (http://www.ngdc.noaa.gov/geomag-web/#igrfwmm, last accessed 10 February 2016) with the international geomagnetic reference field (IGRF10, Finlay *et al.* 2010). Both directions agree very well and lie inside the 95 per cent confidence limit of the archaeomagnetic direction. Accordingly, well oriented archaeomagnetic samples can provide a precise and accurate reading of the field direction.

Rock magnetism

NRM intensity, bulk susceptibility and Koenigsberger ratios (Fig. 4a, Table 2) do not show a large variation for most specimens, but two groups of specimens lie outside the cluster. Large amounts of plaster account for those specimens with relatively low susceptibility and NRMs but Q-values above 20, while specimens with Q-values below 20 seem to be dominated by different magnetic carriers. Most of these specimens come from two blocks taken in the door reveal. They are different in colour (light red/orange compared to brownish red or grey) and the material and/or oxidation conditions were different for them. This is explained by the different kind of loam, which was used to fix the bricks in the door.

AF and thermal demagnetization provided median destructive field (MDF) and temperature (MDT) values. The MDF values lie for most (82 per cent) specimens between 30 and 60 mT (most around 45 mT) but for two specimens they were about 80 mT and for another two cases they exceeded the maximum (120 mT) field which was used. This points to SD or PSD magnetite as main magnetic carrier but in many specimens also a high coercive mineral, presumably hematite is present because specimens are not demagnetized by 120

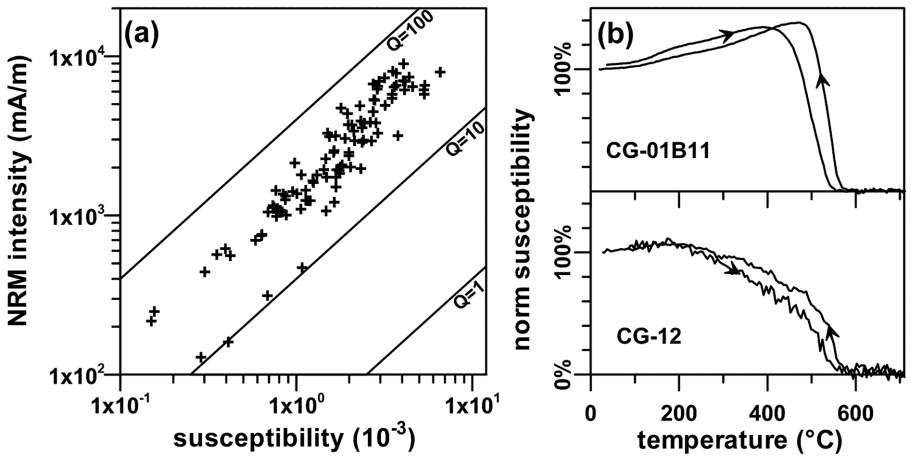

Figure 4. (a) Intensity of natural remanent magnetization (NRM) is plotted versus bulk susceptibility; isolines of Koenigsberger ratio Q are shown. (b) Thermomagnetic curves of susceptibility, heating and cooling is indicated by arrows.

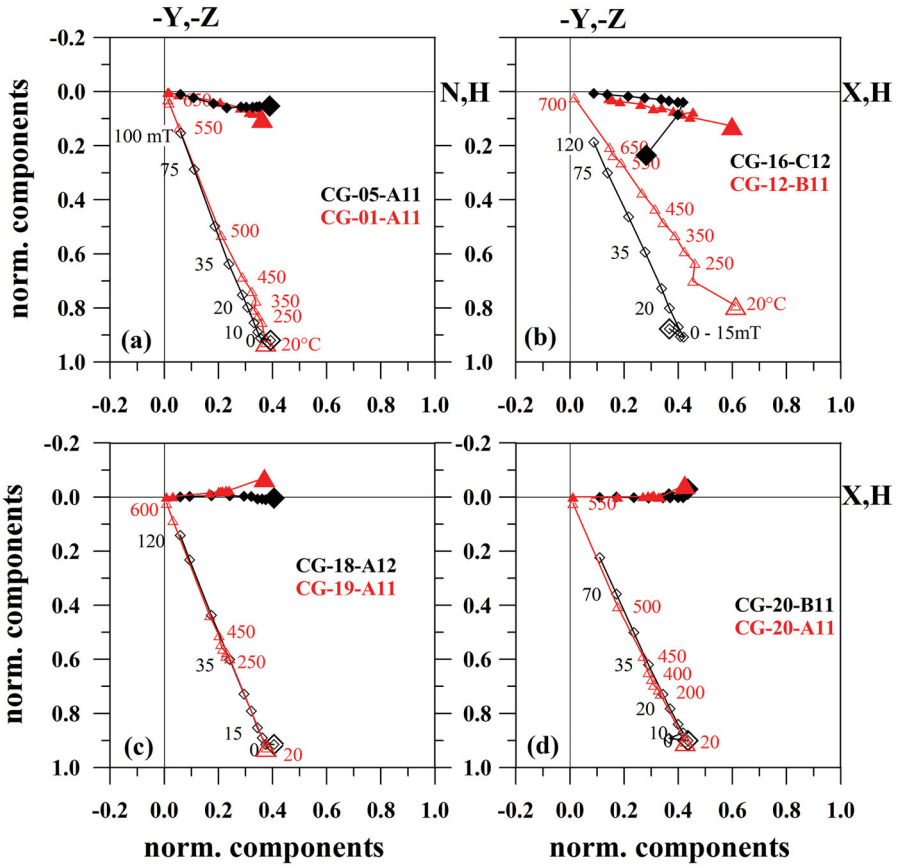

Figure 5. Diagrams of orthogonal vector components normalized to maximum intensity for progressive demagnetization. Red triangles show thermal, black diamonds show AF demagnetization, numbers give demagnetization steps in °C or mT, respectively. Closed symbols are West component (−Y) versus North component (X), open symbols are vertical component (−Z) versus horizontal component (H).

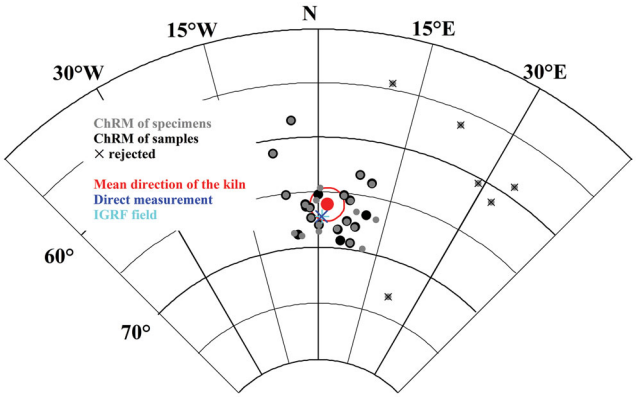

Figure 6. The mean characteristic remanent magnetization directions of specimens, samples and site together with α_{95} are shown in equal area projection. For comparison the direct observation and the IGRF is shown.

mT and preserve in most cases more than 20 per cent of their initial NRM (Fig. 5). The presence of hematite is also supported by thermal demagnetization. Although MDT values lie between 360 and 510 °C for most sister specimens of those with high MDF, during thermal demagnetization they preserve a considerable (10 to 25 per cent) amount of their NRM until 650 °C (Table 2). The magnetic carriers do not contain large amounts of Titanium. This is seen from the absence of field dependence of susceptibility (De Wall 2000), which varies by less than one per cent, when the field is increased from 40 to 400 A m^{-1}. Frequency dependence of susceptibility is low for most specimens and κ_{FD} percentage (Dearing *et al.* 1996) has values between 2 and 3 per cent. Higher values (5–10 per cent) only occur for those specimens which have a strong magnetization component unblocking above 650 °C. Therefore a larger fraction of superparamagnetic grains seems not to be present. Sister specimens of those unblocking at 600 °C have Curie temperatures around 575 °C and a strong susceptibility signal, while the others with a high temperature component have a much weaker susceptibility and more or less continuous unblocking (see Thellier experiments). Nevertheless no pronounced higher Curie temperature can be resolved, but the presence of hematite is indicated by a large amount of magnetization left at the maximum AF field (see Table 2). Thermomagnetic curves of susceptibility show two different types (Fig. 4b), which are nearly reversible. For specimens with strong susceptibility a more or less well pronounced Hopkinson peak is noticed, which is completely absent for those specimens with low susceptibility. Curie temperatures lie between 570 and 594 °C. The observed variation in rock magnetic characteristics is intriguing. There is no evident relationship between unblocking, the position of the samples within the kiln, kind of clay or Koenigsberger ratio. Therefore the reason for this observation remains elusive.

Finally, hysteresis loops obtained from VSM measurements show curves which are not saturated at 1 T (Figs 7a and b: CG-12), and wasp-waisted loops in most cases. In order to resolve the two phases seen from the wasp-waisted loops we plotted the difference between the ascending and descending part of the loop for positive

Table 2. Results of rock magnetic measurements: Specimen name, Koenigsberger ratio, natural remanent magnetization, bulk susceptibility, median destructive field, residuum left at 120 mT, median destructive temperature, residuum left at 600 °C, Curie temperature, frequency dependence of susceptibility κ_{FD}, percentage and absolute after Dearing *et al.* (1996), field dependence of susceptibility (field is increased from 40 to 400 A m^{-1}), remanent coercive force, coercive force, remanent saturation magnetization, saturation magnetization, ratios and kind of hysteresis loop (n = normal, ww = waspwaisted).

Name	Q	NRM ($A\,m^{-1}\,kg^{-1}$)	Kappa ($10^{-3}\,kg^{-1}$)	MDF (mT)	NRM_{ra} (per cent)	MDT (°C)	NRM_{rt} (per cent)	T_c (°C)	κ_{FD} (per cent)	κ_{FD} ($10^{-6}\,m^3\,kg^{-1}$)	κ_{HD} (per cent)	Hcr (mT)	Hc (mT)	Mrs ($Am^2\,kg^{-1}$)	Ms ($Am^2\,kg^{-1}$)	Hcr/Hc	Mrs/Ms	Loop
CG-01A12	34.4	89.9	65.4	42.7	16	508	5	582	2.17	1.47	0.96	46.49	27.17	0.0445	0.1472	1.711	0.302	ww
CG-12B13	18.1	53.4	73.9	>120	67	473	28	573	9.83	7.35	0.19	58.80	28.12	0.0132	0.0560	2.091	0.235	n
CG-17B11	37.6	177.7	118.3	45.5	11	522	3	579	0.63	0.17	0.04	–	–			–	–	–
CG-20B11	43.2	351.0	202.9	56.8	25	486	<3	578	2.27	4.02	0.69	108.17	48.20	0.0883	0.2457	2.244	0.360	ww
CG-22B12	31.7	52.5	41.5	43.5	32	514	33		5.87	1.55	−0							
CG-23B14	32.0	49.4	38.6	83.9	43	361	10	590	6.92	2.43	0.22	100.84	53.96	0.0248	0.0566	1.869	0.438	ww
CG-24B12	36.1	10.8	7.5	>120	57	510	39	585	7.06	0.22	−0.4	–	–			–	–	–
CG-25C12	47.4	264.8	139.7	48.2	10	526	2	574	1.34	1	0.45	–	–			–	–	–
CG-27A11	54.5	106.8	49.0	44.5	26	486	<6	594	1.73	0.78	0.16	54.32	20.44	0.0032	0.0211	2.657	0.153	ww

magnetic field values as ΔM-curve (Tauxe *et al.* 1996) and the derivative of these curves (see Figs 7c and d). If noise of these curves is not taken into account, ΔM-curves show a monotonous decay in all and cases. The derivatives have only one maximum and do not indicate a second high coercive phase, but the decay to zero is rather slow. Although a high coercive mineral component is obviously present, it is concluded that the main magnetic carrier is close to magnetite. Hence, the data tentatively have been plotted in a Day-diagram (Fig. 7e). Three data points plot close to the SD-MD mixing curves of magnetite and in the region of pottery samples (*cf.* Dunlop 2002, fig. 2). The displacement of two points towards the SP-SD mixing curve accounts more likely to the presence of a mineral with high coercivity (*cf.* McIntosh *et al.* 2011) than to the presence of magnetite SP grains. H_{cr}/H_c values ranging from 1.7 to 2.7 are much lower than those observed for the mixtures with that high coercivity mineral (McIntosh *et al.* 2011) or with hematite (Jackson *et al.* 1990). According to the high temperature of unblocking it is hematite.

ARM anisotropy and alteration of its coercivity spectrum was studied for 5 specimens of different blocks. Anisotropy factors ($P = k_1/k_3$, Hrouda 2002) are very low with values between 1.070 and 1.092 and the maximal change of NRM_{ac} direction was 2°. Also alteration of the ARM coecivity spectrum was very weak and it did not exceed 3 per cent with one exception; here it was about 4 per cent (Fig. 8).

Intensity obtained from Thellier experiments

Evaluation of five Thellier experiments was done with the ThellierTool4.2 software (Leonhardt *et al.* 2004) using the default values for classification. Only one specimen passed the automatic routine (Figs 9a–d) and was classified as B because of a large cumulative pTRM check difference δ(pal) and a tail check slightly above the limit of 3 per cent. At 350 °C δ(pal) has a large negative value indicating chemical alteration (Fig. 9d, lower left hand). Nevertheless data points in the Arai-diagram as well as in the Zijderveld-diagram (Figs 9a and b) form straight lines. Using all data points would not change the obtained palaeointensity significantly. This specimen unblocks over a wide range of temperatures and has an almost linear decay of NRM until 480 °C (Fig. 9c). About 30 per cent of the NRM is left at 600 °C indicating also the presence of hematite. The created pTRM is aligned parallel to the laboratory field (Fig. 9d, upper left-hand side) the pTRM-check difference is less than 5 per cent (Fig. 9d, upper right hand). The repeated demagnetization shows very little change except for the last temperature step (Figs. 9c, black squares and d, lower right-hand side). Another specimen (CG-24A11) showed a similar behaviour, but here the tail checks indicated a stronger alteration (Table 3) which was also seen by some distortion of the archaeodirection.

The other three specimens unblock slowly up to temperatures of 450 °C and more than 40 per cent of magnetization was lost in the narrow temperature interval between 540 and 570 °C (Fig. 9g). Accordingly, the data points are clustered in the left part of the Arai-plot and in the Zijderveld-diagrams a considerable scatter is observed for low temperatures (Figs 9e and f). Because of the small amounts of pTRM created during the Thellier experiment large angular differences with respect to H_{Lab} occur (Fig. 9h, upper left-hand side) and no specimen is classified as B. A tentative manual evaluation was performed for temperatures between 100 and 480 °C. Here a well constrained straight line defining palaeointensity was obtained with quality factors (Coe *et al.* 1978) ranging from 1 to 25.

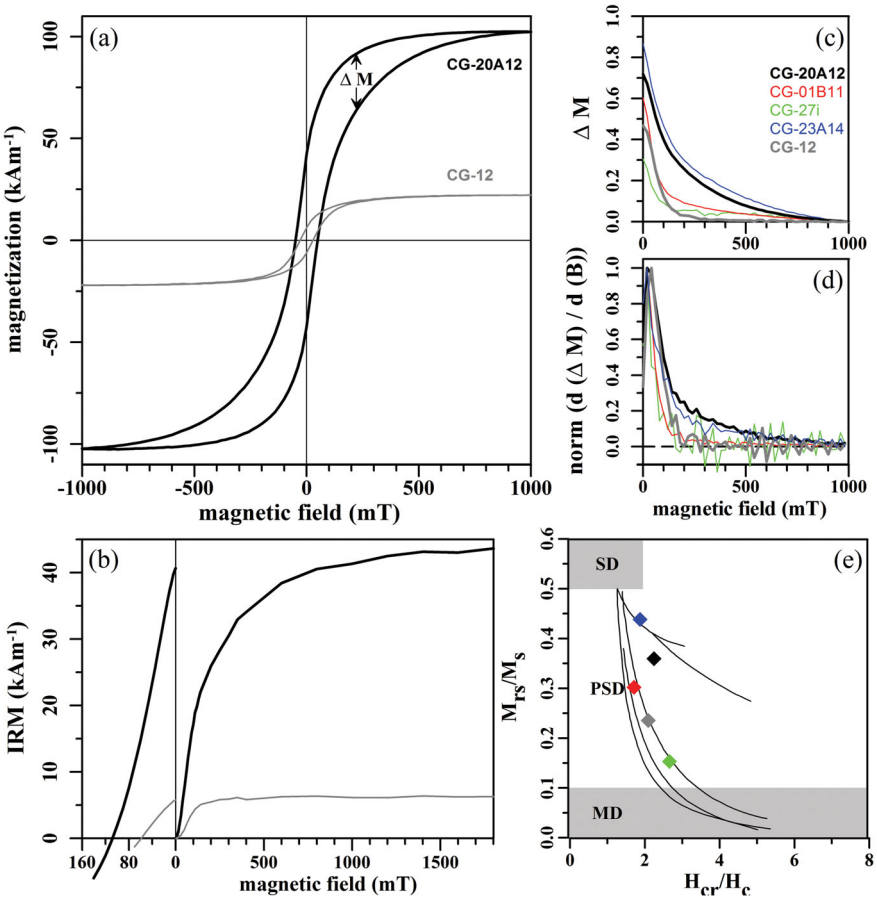

Figure 7. Results of hysteresis measurements provided by (a) apparent hysteresis loops, (b) acquisition of isothermal remanent magnetization (IRM) and back-field curves for two examples. ΔM curve (c, see a and text for definition, Tauxe *et al.* 1996) and the derivative of ΔM (d) are shown and specimen name is indicated. (e) Hysteresis parameters are plotted in a Day diagram (Day *et al.* 1977): ratio of saturation magnetizations is plotted versus ratio of coercivities. The black lines were obtained by Dunlop (2002) for mixtures of SD and MD (three curves left side) or SP and SD (two curves right side) grains.

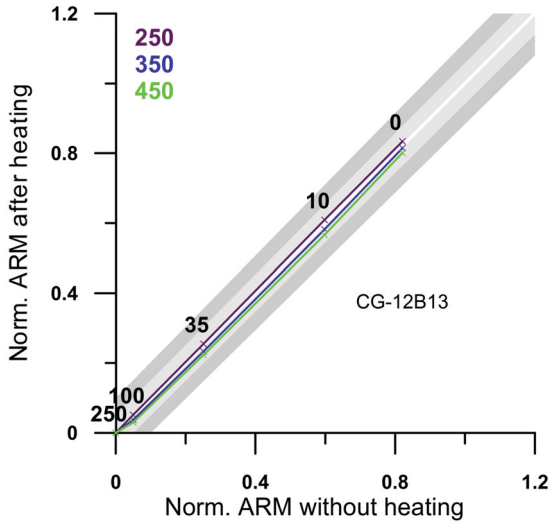

Figure 8. Anhysteretic remanent magnetization demagnetized with four steps (field in mT) after heating to progressive temperatures is plotted versus values of the untreated specimen. Grey shades give 5 and 10 per cent range of change.

After that temperature the pTRM- and additivity-checks indicated a strong alteration. Again alteration was low until about 500 °C; this is in agreement with alteration test for ARM (Fig. 8). The Thellier results rage from 45.14 to 52.11 μT, the unweighted mean of all measurements is 47.98 ± 2.94 μT, which is a relative error of 6.1 per cent (Table 3).

Cooling rate experiments have been carried out at 420 °C/490 °C on three specimens with the technique used by Gómez-Paccard *et al.* (2006). But here, for all three specimens alteration was stronger than cooling rate effect. Accordingly, corrections have not been applied.

Intensity obtained from multiple-specimen experiments

48 specimens prepared from 5 different samples (*cf.* Table 4) have been subjected to the MSP-DSC palaeointensity experiments. As delineated above the MSP-DSC technique could also be interpreted as a multi-specimen palaeointensity experiment with the Dekkers & Böhnel (2006) technique. Here, only the results with NRM fractions between 40 and 60 per cent have been used because the temperature in the DB-steps was not adjusted close to the expected MDT value. This was evaluated by using the TH-step. In order to avoid alteration (see below) lower temperatures have been preferred and thus only six specimens met the criterion. The result is shown in Fig. 10(a). The data points obviously form a straight line and this result looks almost ideal compared to many other published

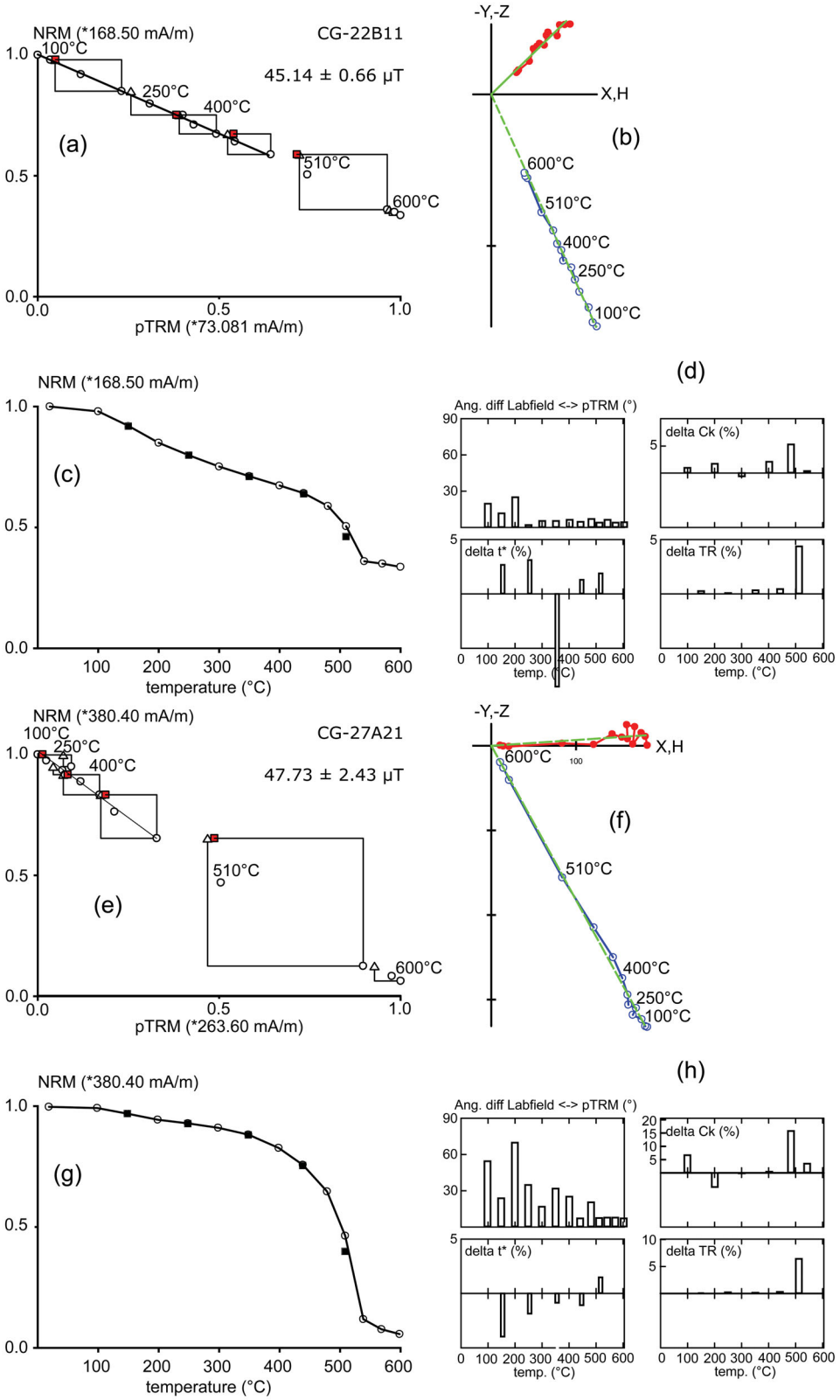

Figure 9. Results of Thellier experiments obtained from Thellier-tool of specimens CG-22B11 (top) and CG-27A21 (bottom) showing (a, e) the Arai plot with pTRM checks as triangles and additivity checks as red squares; (b, f) orthogonal vector components as in Fig. 5 with the calculated mean direction (green line) numbers give temperature steps; (c, g) NRM intensity versus temperature, black squares indicate the results of the repeated demagnetization (TR); (d, h) shows further information as, e.g. pTRM check, error, tail of pTRM*, etc. (see Leonhardt *et al.* 2004 and text).

Table 3. Results of Thellier experiments: Specimen name, laboratory field, palaeointensity and error, minimum and maximum temperatures, number of data points, quality parameters defined by Coe *et al.* (1978) for fraction, gap and quality, by Prévot *et al.* (1985) for weighting, and by Leonhardt *et al.* (2004 and references therein) for classification of the experiment and various checks testing alteration, tails, repeated demagnetization, independency and additivity. The last line gives the un-weighted mean with standard error and number of specimens.

Name	H_{Lab} (μT)	F_{PI} (μT)	σ_F (μT)	T_{min} (°C)	T_{max} (°C)	N	f	g	q	w	Class	CK-error	CK-diff	D_{rat}	d(t*)	d(TR)	d(AC)
CG-17A12	30	49.56	1.35	20	600	14	0.96	0.56	19.5	5.6	C	9.6	15.8	5.2	3.1	12	5.9
CG-22B11	30	45.14	0.66	20	480	10	0.42	0.88	25.0	8.8	B	2	9.5	2.7	3.1	0.4	3.1
CG-24A11	30	52.11	2.16	20	480	10	0.45	0.88	9.5	3.4	C	1.5	9.7	1.7	23.4	0.5	1.9
CG-25A11	30	45.37	5.94	20	480	10	0.17	0.78	1.0	0.3	C	6.5	20.3	21.8	5.1	0.4	2.3
CG-27A21	30	47.73	2.43	20	480	10	0.35	0.8	5.6	2	C	6.4	24.1	9.6	1.5	0.3	1.8
Mean		47.98	2.94	(6.1 per cent)		5											

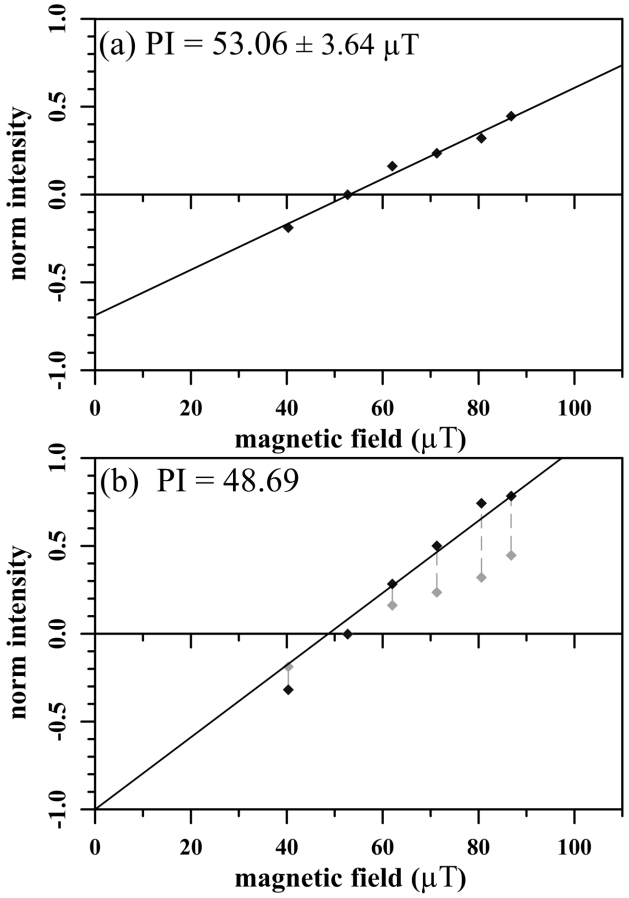

Figure 10. (a) Normalized intensity difference of DB-step plotted versus field together with linear fit line. The data are selected, see text. (b) The same data in grey in comparison with fraction corrected data and their linear fit.

examples (e.g. historic samples of Dekkers & Böhnel 2006; Michalk *et al.* 2008; de Groot *et al.* 2013). The derived palaeointensity result (*cf.* Table 4) is considerably higher than the expected value obtained from the direct measurements. The fraction correction normalizes the created TRM with the part of the NRM, which was replaced by it (see Fabian & Leonhardt 2010; formula 16). Using this correction increases the scatter slightly (Fig. 10b). The line fitted to that data set is anchored at –1 for zero-field. The obtained palaeointensity value is lower and very close to the direct observation (Table 4).

Fig. 11(a) shows the results of all 48 specimens without any correction in comparison with the selection and line discussed above. This figure clearly demonstrates that fractions lower than 40 per cent (see Fig. 11d) introduce a lot of scatter and lead to a clockwise rotation of the DB-line. Hence palaeointensity may be underestimated by using such data. The same effect would occur, if unrecognized alteration would decrease TRM capacity.

Fig. 11(b) shows the same data (a) after application of the correction for fraction, which reduces the dispersion considerably except for relatively high fields. The scatterplot is rotated counterclockwise. The black line was fitted only to those data points which were finally accepted (see below, open black symbols in Fig. 11b). Palaeointensity obtained from this line is slightly lower than the expected field and also lower than the value obtained from a strict application of the DB-method (*cf.* Fig. 10a). The results show that a correct estimation of the MDT value and very homogenous samples are required for application of the DB-method. Otherwise,

Table 4. Results of direct measurement, IGRF and several archaeointensity estimates (see text): n = number of specimens measured, number of specimens used for evaluation, number of samples, correlation coefficient, magnetic field intensity with error (1 sigma).

Method	Fraction used (per cent)	n	N	N_S	r^2	F (μT)
Direct	–	–	–	–	–	48.735
IGRF	–	–	–	–	–	48.830
Thellier	17–96	5	5	5		47.98 ± 2.94
MSP-DB	40–60	–	6	2	0.984	53.06 ± 3.64
MSP-DB fraction corrected	40–60	–	6	2	0.987	48.69
MSP-DSC	25–75	48	17	4	0.998	48.481 ± 0.235
MSP-DSC	20–75	48	24	5	0.996	47.719 ± 0.210

specimens for which fractions deviate strongly from 50 per cent will cause a strong scatter. If fractions are biased to (high) low values, palaeointensity would be (over-) underestimated.

Finally, Fig. 11(c) shows the domain state corrected data (diamonds) with error bars obtained from the RP-step in comparison with the uncorrected data (+). In most cases the DSC is negligible and many error bars are hidden by the symbols. For evaluation of the MSP-DSC-palaeointensity simple selection criteria have been applied, which appear to be reasonable: (1) NRM direction of the specimens must not deviate more than 15° from the axis in which the laboratory field was applied. (2) The fraction used for palaeointensity estimation must range from 25 to 75 per cent of initial NRM and (3) only weak secondary components should be present. Therefore the direction should not change more than 20° for the NRM left after the TH-step. Furthermore the created pTRM must be aligned approximately parallel (<10°) to the applied field. Apart from this, (4) the magnetization obtained in the ZF-step must be smaller than the one obtained in the DB-step. Finally, (5) the RP-step must increase magnetization compared to the ZF-step.

It is worth mentioning that requirements 1–3 demand accurate and reproducible alignment of the specimens' NRM axes with H_{Lab}. Our device allows an accuracy which is less than 5° distortion for declination and 0.5° for inclination. Angular deviations between NRM and demagnetized NRM after the TH-step were with one exception (9°) less than 4°, demonstrating that accurate placing of the specimens is achieved.

Data points plotted in Fig. 11(c) in grey did not meet the above criteria, often because the fraction was too small (d), but also because alteration caused an increase or decrease of TRM capacity. Only 17 of 48 data points are left after application of these very strict criteria, but this provides a very well defined line with a high correlation coefficient ($r = 0.998$). Only three data points deviate from this line, but their contribution is low since they have large error bars. The obtained palaeointensity underestimates the direct value by only 0.5 per cent and this value is in agreement with the direct observation within the 95 per cent error range. Somewhat weaker criteria regarding the accepted fractions (see Table 4, last line) would decrease the error, but also increase the underestimation of palaeointensity to 2 per cent.

The rejected data points show a bias because they lie in most cases above the regression line of the accepted data. Cooling rate effects, which were not taken into account, could be a possible explanation. But SD and small PSD magnetites gain large TRMs after slow cooling, while larger grains do not show such a cooling rate dependence (Ferk *et al.* 2014). By taking the hysteresis parameters into account small grains seem to dominate. The laboratory cooling rate was much faster, less than 1 hr compared to about 16 hr, which were needed for a temperature decrease from 550 to 300 °C during pottery production (*cf.* Fig. 2). Hence, cooling rate effects should cause lower magnetizations and therefore an overestimation of palaeointensity (Yu 2011). Nevertheless, a strong and systematic deviation is not seen in Fig. 11(b) for data points from, for example samples CG-23 and CG-27 (Fig. 7b and c), which may represent different grain sizes. Accordingly, grain size and cooling rate effects do not account for the observed bias.

The scatter of the data points defining the line and the distribution of possible palaeointensity estimates was further investigated with a jackknife resampling technique. The applied technique corresponds to a so called 'delete-d jackknife' for which d values are removed from the original collection of N values. In our case, d is chosen to represent 20 per cent of the collection, which were not taken into account for palaeointensity estimation. Fig. 11(e) shows an almost Gaussian distribution for the selected data set. Additionally, the obtained palaeointensity distribution is shown when data points with fractions of 20–25 per cent are also used. The data set is then supplied with seven additional points (*cf.* Table 4) and this causes the maximum of the slightly bimodal distribution to be shifted to lower values. This results in a considerable underestimation of palaeointensity. Accordingly, it seems that the use of low magnetization fractions of specimens which show alteration can cause an underestimation of palaeointensity. The effect on high fractions could not be investigated, because all specimens which reached more the 58 per cent fraction were rejected because of alteration. Fig. 11(f) summarizes the various palaeointensity estimates and compares with the direct field observation. It shows a good agreement except for the classical DB-experiment. Accordingly, a correction for fraction is recommended. The Thellier results show a large dispersion and single values can be considerably lower or higher than the expected field. Hence, quality criteria demanding at least five independent estimates (i.e. Chauvin *et al.* 2000) are justified.

CONCLUSIONS

An experimental pottery kiln, heated in 2003, was investigated archaeomagnetically. Mean characteristic remanent magnetization direction obtained with standard palaeomagnetic procedures agrees very well with a direct, absolute observation of the field vector obtained one week before operation of the kiln. Thellier experiments as well as the MSP-DSC palaeointensity method provide accurate intensity estimations within their standard deviations. Although the kiln was heated to very high temperatures (>1100 °C) the baked clay is not perfectly stabilized and specimens alter during palaeointensity experiments. The results show that the use of fractions below 25 per cent for the MSP-DSC palaeointensity estimation can cause an underestimation, when alteration occurs. The use of such small fraction should be avoided. The investigation of the MSP-DSC palaeointensity results with a jackknife technique is recommended.

In conclusion the presented investigations show that a pottery kiln is a good recorder of the geomagnetic field vector. The MSP-DSC

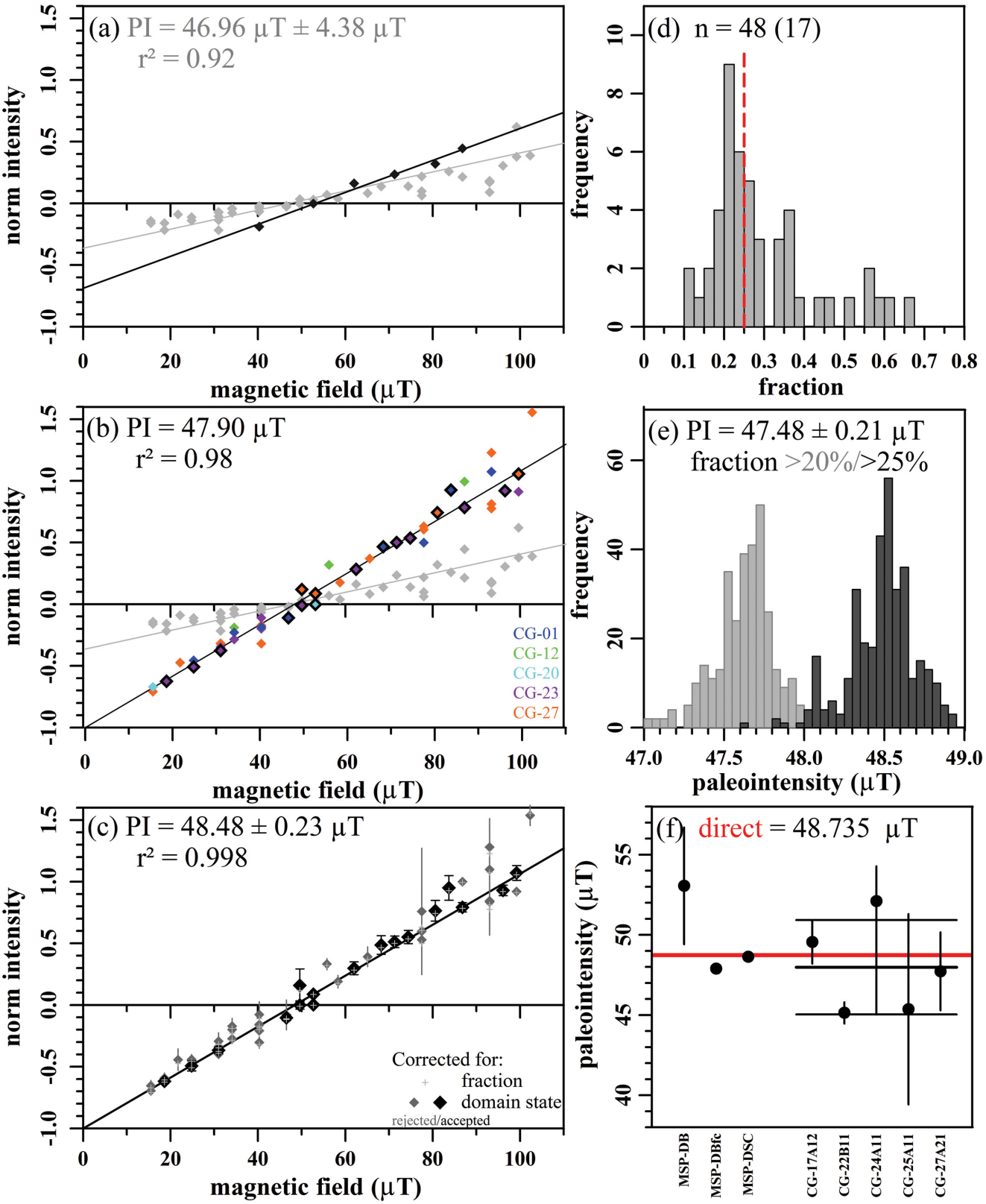

Figure 11. (a) Normalized intensity difference of DB-step plotted versus field without any selection together with linear fit line (grey) and line from Fig. 10(a). (b) The same data in grey in comparison with fraction corrected data and their linear fit line. Colour corresponds to the five samples; specimens with fractions ranging from 25 to 75 per cent are highlighted by black open diamonds. (c) Data from 11(b) (grey +) and corrected for domain state (diamonds) with error bars and linear fit line for selected data (25–75 per cent fraction, black diamonds). (d) Distribution of fractions obtained for all specimens. (e) Distribution of palaeointensity values obtained from jackknife re-sampling technique (see text), only specimens with fractions larger than 25 per cent (20 per cent) were used. (f) Synopsis of all obtained intensity values: direct measurement indicated by red line, from left to right values from Figs 10(a), 11(b), 11(c) and Thellier experiments *cf.* Table 3.

palaeointensity method is able to provide accurate estimates of the field intensity with a very high precision of less than one per cent, when two sigma error margins are used. Nevertheless, caution is recommended when strong alteration occurs and/or many low fraction values are included in palaeointensity estimation. Furthermore the estimation should rely on many (more than ten or fifteen) data points obtained from several samples.

ACKNOWLEDGEMENTS

The study was funded by the Austrian Science Fund (FWF): P23295_N21 (ES) and P24722_N19 (RL). Direct field observations were done in 2003 by M. Fredow and M. Schüler from GFZ. E.S. is indebted to F. Pusterwallner for manufacturing all these complicated sample holders for multiple-specimen palaeointensity. Some rock magnetic measurements were carried out in the palaeomagnetic laboratory of the LIAG at Grubenhagen. Help of S. Scheid and L. Wallbrecht with the VSM is acknowledged. P. Roperch kindly helped in Rennes to carry out some cooling rate experiments.

REFERENCES

Aidona, E., Scholger, R., Mauritsch, H.J. & Perrak, M., 2008. Remanence acquisition in a Roman-style gold furnace, *Phys. Chem. Earth,* **33,** 438–448.

Böhnel, H.N., Dekkers, M.J., Delgado-Argote, L.A. & Gratton, M.N., 2009. Comparison between the microwave and multispecimen parallel difference pTRM paleointensity methods, *Geophys. J. Int.,* **177,** 383–394.

Brosch, R., Klett-Drechsel, J., König, S., Krabath, S. & Stephan, H.-G., 2003. Steinzeug wie aus dem Mittelalter, *Archäologie in Niedersachsen,* **6,** 136–139.

Catanzariti, G., McIntosh, G., Gómez-Paccard, M., Ruiz-Martínez, V.C., Osete, M.L., Chauvin, A. & Team, T.A.S., 2008. Quality control of archaeomagnetic determination using a modern kiln with a complex NRM, *Phys. Chem. Earth,* **33,** 427–437.

Chauvin, A., Garcia, Y., Lanos, P. & Laubenheimer, F., 2000. Paleointensity of the geomagnetic field recorded on archaeomagnetic sites from France, *Phys. Earth Planet. Int.,* **120,** 111–136.

Coe, R.S., 1967. Paleointensities of the Earth's magnetic field determined from Tertiary and Quaternary rocks, *J. geophys. Res.,* **72,** 3247–3262.

Coe, R.S., Grommé, S.C. & Mankinen, E.A., 1978. Geomagnetic paleointensities from radiocarbon-dated lava flows on Hawaii and the question of the Pacific nondipole low, *J. geophys. Res.,* **83,** 1740–1756.

Cromwell, G., Tauxe, L., Staudigel, H. & Ron, H., 2015. Paleointensity estimates from historic and modern Hawaiian lava flows using glassy basalt as a primary source material, *Phys. Earth planet. Int.,* **241,** 44–56.

Day, R., Fuller, M. & Schmidt, V.A., 1977. Hysteresis properties of titanomagnetites: grain-size and compositional dependence, *Phys. Earth planet. Int.,* **13,** 260–267.

de Groot, L.V., Mullender, T.A.T. & Dekkers, M.J., 2013. An evaluation of the influence of the experimental cooling rate along with other thermomagnetic effects to explain anomalously low palaeointensities obtained for historic lavas of Mt Etna (Italy), *Geophys. J. Int.,* **193,** 1198–1215.

De Wall, H., 2000. The field-dependence of AC susceptibility in titanomagnetites: implications for the anisotropy of magnetic susceptibility, *Geophys. Res. Lett.,* **27,** 2409–2411.

Dearing, J.A., Dann, R.J.L., Hay, K., Lees, J.A., Loveland, P.J., Maher, B.A. & O'Grady, K., 1996. Frequency-dependent susceptibility measurements of environmental materials, *Geophys. J. Int.,* **124,** 228–240.

Dekkers, M.J. & Böhnel, H.N., 2006. Reliable absolute palaeointensities independent of magnetic domain state, *Earth planet. Sci. Lett.,* **248,** 508–517.

Dunlop, D., 2002. Theory and application of the Day plot (M_{rs}/M_s versus H_{cr}/H_c): 2., Application to data for rocks, sediments and soils, *J. geophys. Res.,* **107,** 2057, doi:10.1029/2001JB000487.

Fabian, K. & Leonhardt, R., 2010. Multiple-specimen absolute paleointensity determination: an optimal protocol including pTRM normalization, domain-state correction, and alteration test, *Earth planet. Sci. Lett.,* **297,** 84–94.

Ferk, A., Denton, J.S., Leonhardt, R., Tuffen, H., Koch, S., Hess, K.-U. & Dingwell, D.B., 2012. Paleointensity on volcanic glass of varying hydration states, *Phys. Earth planet. Int.,* **208–209,** 25–37.

Ferk, A., Leonhardt, R., Hess, K.-U., Koch, S., Egli, R., Krása, D. & Dingwell, D.B., 2014. Influence of cooling rate on thermoremanence of magnetite grains: identifying the role of different magnetic domain states, *J. geophys. Res.,* **119,** 1599–1606.

Finlay, C.C. *et al.*, 2010. International Geomagnetic Reference Field: the eleventh generation, *Geophys. J. Int.,* **183,** 1216–1230.

Genevey, A. & Gallet, Y., 2002. Intensity of the geomagnetic field in Western Europe over the past 2000 years: new data from ancient French pottery, *J. geophys. Res.,* **107**(B11), 2285, doi:10.1029/2001JB000701.

Gómez-Paccard, M., Chauvin, A., Lanos, P., Thiriot, J. & Jiménez-Castillo, P., 2006. Archeomagnetic study of seven contemporaneous kilns from Murcia (Spain), *Phys. Earth planet. Int.,* **157,** 16–32.

Herrero-Bervera, E. & Valet, J.-P., 2009. Testing determinations of absolute paleointensity from the 1955 and 1960 Hawaiian flows, *Earth planet. Sci. Lett.,* **287,** 420–433.

Hrouda, F., 2002. The use of the anisotropy of magnetic remanence in the resolution of the anisotropy of magnetic susceptibility into its ferromagnetic and paramagnetic components, *Tectonophysics,* **347,** 269–281.

Jackson, M., Worm, H.-U. & Banerjee, S.K., 1990. Fourier analysis of digital hystesis data: rock magnetic applications, *Phys. Earth planet. Int.,* **65,** 78–87.

Jankowski, J. & Sucksdorff, C., 1996. *Guide for Magnetic Measurements and Observatory Practice*, International Association of Geomagnetism and Aeronomy.

Kirschvink, J.L., 1980. The least squares line and plane and the analysis of paleomagnetic data, *Geophys. J. R. astr. Soc.,* **62,** 699–718.

Krása, D., Heunemann, C., Leonhardt, R. & Petersen, N., 2003. Experimental procedure to detect multidomain remanence during Thellier–Thellier experiments, *Phys. Chem. Earth,* **28,** 681–687.

Leonhardt, R., Heunemann, C. & Kása, D., 2004. Analyzing absolute paleointensity determinations: acceptance criteria and the software ThellierTool4.0, *Geochem. Geophys. Geosyst.,* **5,** Q12016, doi:10.1029/2004GC000807.

McFadden, P.L., 1982. Rejection of palaeomagnetic observations, *Earth planet. Sci. Lett.,* **61,** 392–395.

McIntosh, G., Kovacheva, M., Catanzariti, G., Donadini, F. & Osete Lopez, M.L., 2011. High coercivity remanence in baked clay materials used in archeomagnetism, *Geophys. Geochem. Geosyst.,* **12,** Q02003, doi:10.1029/10.1029/2010GC003310.

Michalk, D.M., Muxworthy, A.R., Böhnel, H.N., Maclennan, J. & Nowaczyk, N., 2008. Evaluation of the multispecimen parallel differential pTRM method: a test on historical lavas from Iceland and Mexico, *Geophys. J. Int.,* **173,** 409–420.

Morales, J., Goguitchaichvili, A., Aguilar-Reyes, B., Pineda-Duran, M., Camps, P., Carvallo, C. & Calvo-Rathert, M., 2011. Are ceramics and bricks reliable absolute geomagnetic intensity carriers?, *Phys. Earth planet. Int.,* **187,** 310–321.

Nakajima, T., Torii, M., Natsuhara, N., Yaskawa, K., Takagi, M., Ikeguchi, K. & Kawai, N., 1974. Remanent magnetism of the reconstructed ancient kiln, *Rock Magn. Paleogeophy.,* **2,** 28–31.

Newitt, L.R., Barton, C.E. & Bitterly, J., 1996. *Guide for Magnetic Repeat Station Surveys*, International Association of Geomagnetism and Aeronomy.

Prévot, M., Mankinen, E.A., Coe, R.S. & Grommé, C.S., 1985. The Steens Mountain (Oregon) geomagnetic polarity transition, 2. Field intensity variations and discussion of reversal models, *J. geophys. Res.,* **90,** 10 417–10 448.

Riisager, P. & Riisager, J., 2001. Detecting multidomain magentic grains in Thellier paleointensity experiments, *Phys. Earth Planet. Int.,* **125,** 111–117.

Schnepp, E., Pucher, R., Reinders, J., Hambach, U., Soffel, H.C. & Hedley, I., 2004. A German catalogue of archaeomagnetic data, *Geophys. J. Int.,* **157,** 64–78.

Schnepp, E., Worm, K. & Scholger, R., 2008. Improved sampling techniques for baked clay and soft sediments, *Phys. Chem. Earth,* **33,** 407–413.

Soffel, H.C. & Schurr, K., 1990. Magnetic refraction studied on two experimental kilns, *Geophys. J. Int.,* **102,** 551–562.

Stephan, H.-G., 2010. *Der Solling im Mittelalter*. Hallesche Beiträge zur Archäologie des Mittelalters und der Neuzeit, 1, pp. 600, archaeotopos-Verlag, Dormagen.

Tanguy, J.-C., Le Goff, M., Principe, C., Arrighi, S., Chillemi, V., Paiotti, A., La Delfa, S. & Patanè, G., 2003. Archeomagnetic dating of Mediterranean volcanics of the last 2100 years: validity and limits, *Earth Planet. Sci. Lett.,* **211,** 111–124.

Tauxe, L., Mullender, T.A.T. & Pick, T., 1996. Potbellies, wasp-waists, and superparamagnetism in magnetic hysteresis, *J. geophys. Res.,* **101,** 571–583.

Veitch, R.J., Hedley, G. & Wagner, J.J., 1984. An investigation of the intensity of the geomagnetic field during Roman times using magnetically anisotropic bricks and tiles, *Arch. Sc. Genève,* **37,** 359–373.

Yamamoto, Y., Torii, M. & Natsuhara, N., 2015. Archeointensity study on baked clay samples taken from the reconstructed ancient kiln: implication for validity of the Tsunakawa-Shaw paleointensity method, *Earth, Planets, Space,* **67,** 63–76.

Yu, Y., 2011. Importance of cooling rate dependence of thermoremanence in paleointensity determination, *J. geophys. Res.,* **116,** B09101, doi:10.1029/2011JB008388.